Robustness and stability of flow-and-diffusion structures

David G. Míguez,[1,*] Gonzalo G. Izús,[2] and Alberto P. Muñuzuri[1]
[1]*Chemistry Department, Brandeis University, Waltham, Massachusetts 02454, USA*
[2]*Departamento de Física, Facultad de Ciencias Exactas y Naturales, Universidad Nacional de Mar del Plata and CONICET, Deán Funes 3350, 7600 Mar del Plata, Argentina*
[3]*Group of Complex Systems, Universidade de Santiago de Compostela, 15782 Santiago de Compostela, Spain*
(Received 3 March 2005; published 11 January 2006)

Reaction-diffusion-advection systems have revealed an interesting variety of pattern formation mechanism during the last years. Inside this field, flow-and-diffusion structures (FDSs) appear as a generalization of the mechanism of spatial symmetry breaking for different diffusion coefficients and flow rates of activator and inhibitor. The recent experimental validation of FDSs situates these structures in the focus of the actual research. We will report here an experimental and numerical analysis of the theoretically predicted robustness of these flow-and-diffusion structures by using different boundary profiles of illumination used to obtain FDSs. The results here shown reveal important characteristics related with the coexistence and interaction between these structures.

DOI: 10.1103/PhysRevE.73.016207 PACS number(s): 89.75.Fb

I. INTRODUCTION

The problem of reaction-diffusion systems subjected to flow influence is one of the most interesting and unexplored topics in nonlinear science. Initially, research was focused in to avoid convective effects in stirred reactors [1–4]. But nowadays research is mainly focused on the combination of both reaction diffusion and convection to explore different ways of interaction and pattern formation [5–8]. The mixture of self-organization and advection is closely related with processes of growth and embryo development in living organisms. The idea of a morphogen traveling through the embryo as a cause of the cell specialization was primary proposed by Murray [9]. Recent research has demonstrated the existence of gene expression oscillations which, combined with flow, determine crucial aspects in the vertebrae formation [10–12]. The effect of advection in chemical and biological steady patterns determines their final spatial configuration [13]. In addition, successful attempts to combine convective and chemical patterns were performed [14].

Pattern-forming systems under the influence of chemical flow has been observed to support self-sustained structures [34–36]. The interest here resides in the fact that now the convection is responsible for the stabilization of stationary chemical gradients [15]. The arising structure is periodic in the direction of the flow, and the wavelength is determined by the velocity of the flow. These stationary structures, baptized as FDOs (flow-distributed oscillations) were experimentally obtained by Menzinger and co-workers [6]. This discovery has not been absent of controversy, due to the apparent simplicity of the underlying mechanism [16,17].

Another kind of structure generalizes the mechanism to systems with different flow rates and diffusion coefficients [7,18–20]. Flow-and-diffusion structures (FDSs) constitute the generalization of the Turing mechanism for the more general reaction-diffusion-advection system. Chemical species can flow with general velocities and diffusion rates [21]. This way, Turing instability [22] can be understood as a limit case for FDS when advection equals zero.

The conceptual idea is that an advective boundary can destabilize the medium, creating a spatially periodic steady pattern. This purely convective instability occurs when the flow velocity reaches a threshold value. This threshold separates the absolute unstable regime and the convective unstable regime and it is determined by the chemical conditions of the particular system [23]. When the system is in the absolute unstable regime (i.e., flow velocity is below the threshold) the dynamics of the system is dominated by normal phase waves of Hopf oscillations. Once the convective unstable regime is reached, a periodic steady structure arises in the direction of the flow. This pattern is composed by spatial periodic modulations in the concentration of activator and inhibitor, with a wavelength that depends both on chemical and dynamical aspects. This pattern corresponds to the FDS instability. Flow-and-diffusion structures are predicted to be very robust and general, in the sense that the same instability has been found for many theoretical models [19,24].

Experimental evidence of flow-and-diffusion structures was carried out by using the standard equivalence between a feeding boundary and a moving mask of illumination [25,26]. This system has the additional advantage that no turbulence is present due to the advection, so the flow is ensured to be directional. In addition, experiments can be performed in open chemical reactors using gels. This way, the pattern FDS will be steady with respect to the traveling boundary, in concordance with the purely convective situation.

In order to corroborate the theoretical predictions about the robustness and stability of FDSs, experiments and numerical simulations with different kinds of moving boundaries were performed. The goal is to check the structural stability of the steady FDSs by varying the geometry of the

*URL: http://people.brandeis.edu/~miguez/; electronic address: miguez@brandeis.edu

boundary. In addition, experiments showing key aspects in the interaction between two FDSs are reported.

II. EXPERIMENTAL SETUP

Experiments on the photosensitive CDIMA (chlorine dioxide, iodine, malonic acid) reaction [27,28] were performed in a thermostatic continuously fed unstirred one-feeding-chamber reactor (CFUR) [29,30] at 4 ± 0.5 °C. We observe two-dimensional patterns in an Agarose gel layer (2% agarose, 0.3-mm thickness, 20-mm diameter). To ensure the two-dimensionality of the structure, the thickness of the gel was kept less than the wavelength exhibited by the system for the concentrations used here. Two membranes were placed between the gel and the feeding chamber: a nitrocellulose membrane (Schleicher & Schnell, pore size 0.45 mm) and an Anapore membrane impregnated with 0.5% agarose gel (Whatman, pore size 0.2 μm).

The reagents were fed into the CSTR by a peristaltic pump, previously calibrated to ensure the correct control in the concentrations value. The input concentration of reagents were $[ClO_2]=0.15$ mM, $[I_2]=0.45$ mM, $[H_2SO_4]=10$ mM, and [malonic acid]$=1.2$ mM. The residence time of the reactants in the reactor was fixed at $T=125$ s. We add [PVA] $=0.5$ mM, as an indicator of the activator concentration. This way, parts with high activator concentration exhibit garnet coloration, and parts with inhibitor dominance show light yellow color. In addition, polyvinyl alcohol (PVA) concentration controls the ratio between diffusion coefficients of activator and inhibitor. Varying its value, Turing structures (high concentration) or oscillations (low concentration) can be obtained with this CDIMA reaction [31,32]. Illumination was provided using a video projector (Hitachi, CP-X327) focused onto the gel and connected to a computer. Under this circumstance, the system itself may exhibit oscillations (see Fig. 1) for low intensity of illumination and steady state for large illumination values.

A typical experiment consists of the following: under the conditions explained before, and starting with homogeneous and high light intensity, a boundary of illumination begins to travel through the medium with constant velocity. This way, the illuminated zone (steady state) decreases its size, to the expense of the growth of the region in shadow which, in the stationary case, is in Hopf domain. This situation is an analog to the feeding boundary system. If the observer is moving with the velocity of the boundary, he will see a constant flow of reactants through the boundary [33].

When a steplike boundary separating steady and oscillatory regions propagates throughout the medium with sufficiently large velocity, a pattern of parallel stripes (FDSs) appears covering the medium behind the boundary. The minimum velocity for the formation of FDSs is estimated as $V_{exp}=3.1\pm0.5$ mm/h. Different geometries of the boundary were considered in order to check their influence on FDS properties. The different moving boundaries of illumination were produced by a self-developed program, simply focusing the video projector onto the medium and projecting whatever image was produced in the computer. This allows us to easily explore different possibilities of formation of FDSs.

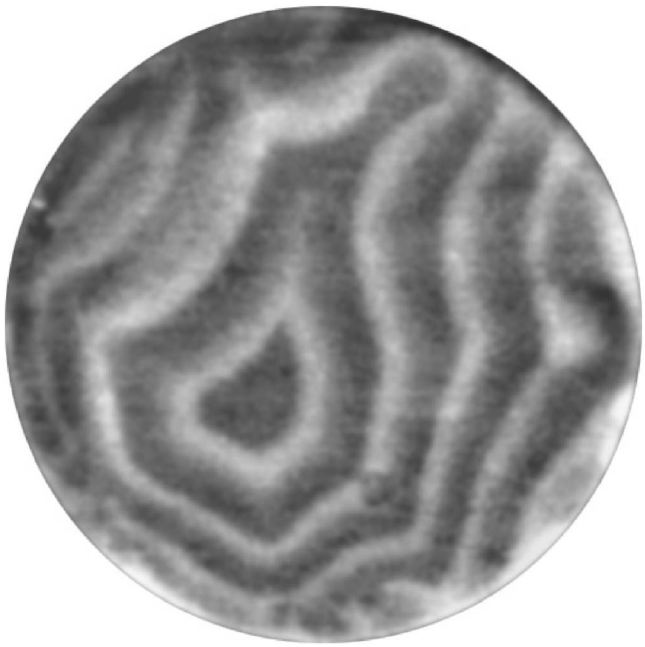

FIG. 1. Phase waves formed in the CDIMA reaction under oscillatory condition for low intensity of illumination. The wavelength of the structure is $\lambda=2.9\pm0.6$ mm.

III. NUMERICAL SIMULATIONS

To validate the experimental results, numerical simulations were performed using the Lengyel-Epstein model for the CDIMA reaction [31]. In the case of a space and time-dependent light intensity $\phi(x,y,t)$, the CDIMA rate equations are described by the two-variable Lengyel-Epstein reaction-diffusion scheme:

$$\frac{\partial u}{\partial t} = a - cu - \frac{4uv}{1+u^2} - \phi + \nabla^2 u,$$

$$\frac{\partial v}{\partial t} = \sigma\left(cu - \frac{uv}{1+u^2} + \phi + D_v\nabla^2 v\right). \tag{1}$$

Here u and v are the dimensionless concentrations of the activator and the inhibitor key species, respectively; a, c, and σ are dimensionless parameters related to other initial concentrations and rate constants, and D_v is proportional to the ratio of diffusion coefficients. The uniform steady state $S=(u_s,v_s)$ is given by

$$S = \left(\frac{a-5\phi_0}{5c},\ \frac{a(1+u_s^2)}{5u_s}\right) \tag{2}$$

that exists for homogeneous illumination in the parameter regime $a \geqslant 5\phi_0$ and $c \geqslant 0$, while stable homogeneous oscillations are a solution of Eqs. (1) for $a \leqslant 5\phi_0$. Both states can coexist in a stable way under a suitable stationary illumination profile.

Numerical results are obtained through the integration of Eqs. (1) in one and two spatial dimension with a finite difference scheme. We consider a rectangular CFUR with lengths L_x and L_y and nonflux boundary conditions are as-

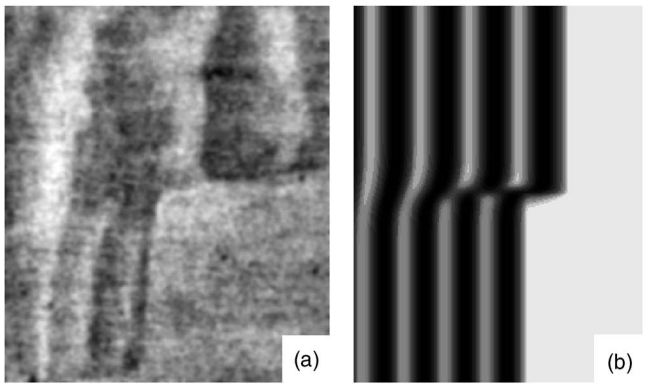

FIG. 2. Snapshot of the experiment (a) and numerical simulation (b) corresponding to the case of double velocity in the moving boundary. Velocities used were (a) $V_1=4$ mm/h and $V_2=8$ mm/h, (b) $V_1=10$ s.u./t.u. and $V_2=12$ s.u./t.u. Size of (a)=10 $\times 10$ mm. The mask is moving from left to right.

sumed at $x=0,L_x$ and $y=0,L_y$. Lengths $L_{x,y}$ are chosen in order to allow any FDS to be completely developed before it reaches the end of the CFUR. For similitude with experiments, our simulations were performed using a moving boundary of illumination, but the same results can be obtained when an advection term is considered in Eq. (1).

Hereafter, we fix some parameter values to the following: $a=22$, $c=1.3$, $d=1.07$, and $\sigma=5$ in order to reproduce experimental conditions far from the Turing bifurcation. The illumination varies between two values: in the low-illuminated region ($\phi_0=2$) the uniform solution of the system is inside the Hopf domain, and in the high-illuminated region ($\phi_0=4$) the solution is the uniform steady state S. Under these conditions, the threshold velocity for the FDS formation in the simulation is estimated numerically, $v_{num}=7.2\pm0.5$ space units/time units (s.u./t.u.).

IV. RESULTS

The starting point we wanted to verify concerns the stability of the two-dimensional arrangement of FDSs. In such a sense, two FDSs with different wavelengths are imposed in the same system. To do that, we developed a program that projects two moving boundaries into the medium (the velocity of one being double that of the other's). This way, we produce two different FDSs coexisting in the same region. Numerically we have used the external illumination profile $\phi(x,y,t)=3+H[x-x_0-v_{el}(y)t]+\xi(x,y,t)$, where $H(z)$ is a step function: $H(z)=-1(+1)$ if $z\leqslant 0$ ($\geqslant 0$), x_0 is the initial location of the illumination boundary and $v_{el}(y)$ is a piecewise constant velocity $v_{el}(y)=v_1$ if $y\leqslant L_y/2$ and $v_{el}(y)=v_2$ for $y\geqslant L_y/2$. $\xi(x,y,t)$ is a real Gaussian white noise of intensity ϵ, with zero mean and δ correlated in space and time. This low intensity noise in the illumination was introduced to mimic the intrinsic noise present in all experiments, but it did not produce an appreciable change in the final shape and behavior of the patterns[34].

The experimental result is shown in Fig. 2(a) while the numerical simulation is plotted in Fig. 2(b). The coexistence

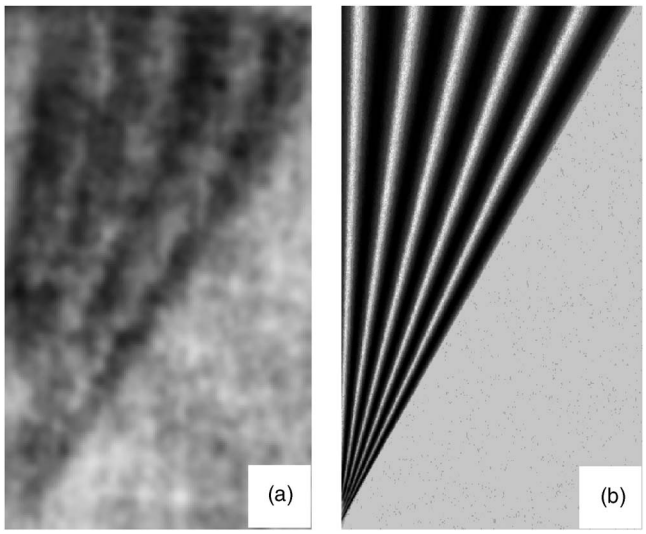

FIG. 3. Snapshots of FDSs obtained from a mask of illumination with a y-dependent velocity of propagation. (a) Correspond to experimental results, and (b) is a numerical simulation with the same kind of moving mask. It can be observed that the coexistence of a continuum value in the wavelength is also possible. For v_{el} below the FDS threshold convective propagating structures are developed. The mask is moving from left to right. Velocity on the top: (a) $V=8$ mm/h, (b) $V=12$ s.u./t.u.

of two stable FDSs in the low illuminated region is appreciated. The boundary between both FDSs at $y=L_y/2$ is determined by the geometry of the mask of illumination and it remains stable during the time evolution, even in the presence of a source of noise and diffusive transport. These experiments show that FDSs can coexist with different wavelengths, even when the values for the wavelengths are extremely different.

In this way, we have also constructed a traveling mask that induces in experiments a pattern whose wavelength is continuously varied. Thus we projected a boundary onto the system whose velocity depends linearly with the value of Y. Here the CFUR is forced by a profile of illumination with velocity $v_{el}(y)=v_{el}y/L_y$. The analogy with the purely advective system is a feeding boundary with different flow velocities in each point.

The results of the experiment and the corresponding numerical simulation are shown in Fig. 3. From Fourier analysis of the numerically obtained patterns we conclude that a FDS with a continuum value of wavelengths is maintained. The wavelength, understood as the periodicity in the X direction, goes from small values on the bottom to very large values on the top. The lower part of both figures is not clearly defined, because we are in the range of velocities below the critical value for FDS formation.

The next goal is to check the robustness of the pattern for geometrical changes. The study of the behavior of the FDS for different shapes of the boundaries will report an intuitive idea of their underlying properties. In addition, we can prove this way the interesting nature of this kind of pattern, completely different from the purely Hopf oscillations, which would correspond to these parameter values without advection.

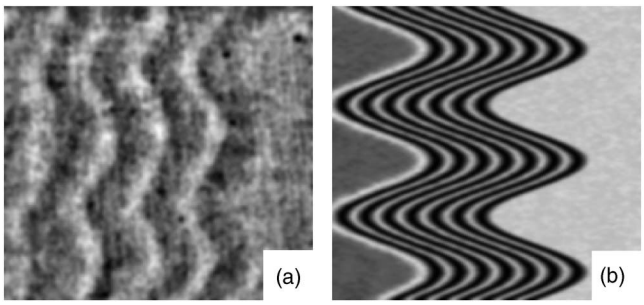

FIG. 4. Snapshot of a FDS obtained with a mask of illumination modulated along y. (a) Experimental ($V=5.0\pm0.1$ mm/h) and (b) numerical simulation ($V=12$ s.u./t.u.) shows that the FDS configuration is marked by the configuration of the boundary. The mask is moving from left to right.

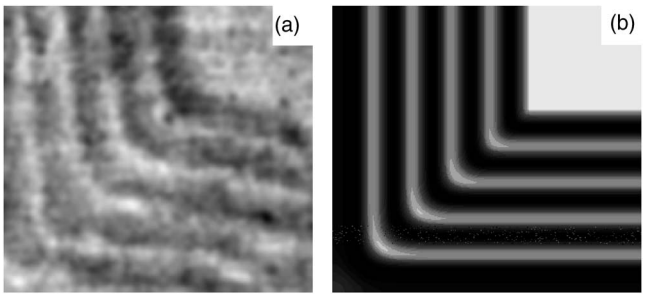

FIG. 5. Interacting perpendicular FDSs generated by two boundaries of light moving in a perpendicular way. (a) is the experimental result ($V=5.0\pm0.1$ mm/h) and (b) is the corresponding numerical simulation ($V=12$ s.u./t.u.). One mask is moving from left to right and the other from bottom to top, both with the same velocity.

To do that, we perform a mask with a sinusoidal profile, as an illustrative example. To explore this property numerically, we have also considered space-periodic profiles of illumination $\phi(x,y,t)=3+H[x-x_d(y)-v_{el}t]+\xi(x,y,t)$, where $x_d=x_0+\delta\sin(ky)$. Figure 4 strongly suggests that the properties of the external illumination determines the shape of FDSs which follows adiabatically the mask of illumination. Both, experimental and numerical system behaves exactly in the same way: each stripe appears with the same shape as the one used in the mask. The wavelength is not affected and the pattern remains with this imposed geometry far from the boundary of light. Again, the flux influence stabilizes the configuration of the FDS, maintaining a pattern that mimics the shape of the feeding boundary.

Finally, another important issue is to study the collision between different FDSs, in order to check the interaction of two of these waves. We use a mask composed of two boundaries moving in a perpendicular arrangement, in the form of a rectangle of high light intensity traveling through the medium. The analogous case in the purely convective system is composed of two feeding boundaries situated forming an angle of $\pi/2$. In the simplest case the two boundaries are moving with the same velocity, so both interacting FDSs have the same wavelength, although similar results are obtained when velocities are not equal.

Figure 5 shows these results. Vertical and horizontal waves collide in the diagonal marked by the displacement of both boundaries. As time goes on, the interaction results in annihilation of the pattern after the collision. The final structure is composed by two sets of perpendicular FDSs linked at the collision point. In spite of the apparent simplicity of the idea (two perpendicular boundaries with the same advection velocities), the interaction of FDSs reveals a quite complicated mechanism, that needs a more detailed analysis.

V. CONCLUSION

In this paper, we report an analysis of the robustness and structural stability of FDSs in front of changes in the shape of the boundary of illumination. For all cases reported here, the geometry of the FDSs is closely determined by the moving boundary as well as the wavelength given by the boundary velocity. Also we investigate the coexistence of different wavelengths and the interaction between FDSs. After visualizing all the results, one can conclude that these mechanisms of formation of steady patterns is extremely robust. This strong stability and robustness is, by itself, one of the key arguments for these structures to be a serious candidate to explain the underlying mechanism in some biological segmentation processes.

ACKNOWLEDGMENTS

G. Izús acknowledges the Spanish Ministry of Foreign Affairs (MAE-AECI Program) and to the Universidade de Santiago de Compostela (Grupo de Sistemas Complexos) for the kind hospitality. All numerical computations were performed at the Centro de Supercomputación de Galicia CESGA (Spain).

[1] J. A. Vastano, J. E. Pearson, W. Horsthemke, and H. L. Swinney, J. Chem. Phys. **88**, 6157 (1988).
[2] G. Kshirsagar, Z. Noszticzius, W. D. McCormick, and H. L. Swinney, Physica D **49**, 5 (1991).
[3] R. D. Vigil, Q. Ouyang, and H. L. Swinney, Physica A **188**, 17 (1991).
[4] F. Ali and M. Menzinger, J. Phys. Chem. **101**, 2304 (1997).
[5] A. B. Rovinsky and M. Menzinger, Phys. Rev. Lett. **70**, 778 (1993).
[6] Mads Kærn and Michael Menzinger, Phys. Rev. E **60**, R3471 (1999).
[7] R. A. Satnoianu, P. K. Maini, and M. Menzinger, Physica D **160**, 79 (2001).
[8] M. Kærn, M. Menzinger, R. A. Satnoianu, and A. Hunding, Faraday Discuss. **120**, 295 (2001).
[9] J. D. Murray, *Mathematical Biology* (Springer Verlag, Berlin,

1989).
[10] M. Kærn, M. Menzinger, and A. Hunding, J. Theor. Biol. **207**, 473 (2000).
[11] I. K. Quigley and D. M. Parichy, Microsc. Res. Tech. **58**, 442 (2002).
[12] M. Kærn, D. G. Míguez, A. P. Muñuzuri, and M. Menzinger, Biophys. Chem. **110**, 231 (2004).
[13] D. G. Míguez, M. Dolnik, and A. P. Muñuzuri, Phys. Rev. Lett. (to be published).
[14] I. Deza, A. P. Muñuzuri, V. Pérez-Muñuzuri, and V. Pérez-Villar (unpublished).
[15] P. Andresén, M. Bache, E. Mosekilde, G. Dewel, and P. Borckmans, Phys. Rev. E **60**, 297 (1999).
[16] P. Andresén, E. Mosekilde, G. Dewel, and P. Borckmans, Phys. Rev. E **62**, 2992 (2000).
[17] M. Kærn and M. Menzinger, Phys. Rev. E **62**, 2994 (2000).
[18] R. A. Satnoianu and M. Menzinger, Phys. Rev. E **62**, 113 (2000).
[19] R. A. Satnoianu and M. Menzinger, Phys. Lett. A **304**, 149 (2002).
[20] R. A. Satnoianu, Phys. Rev. E **68**, 032101(2003).
[21] R. A. Satnoianu, UK Nonlinear News **28**, 1 (2002).
[22] A. M. Turing, Philos. Trans. R. Soc. London, Ser. A **327**, 31 (1952).
[23] S. P. Kuznestov, E. Mosekilde, G. Dewel, and P. Borckmans, J. Chem. Phys. **106**, 7609 (1997).
[24] P. V. Kuptsov and R. A. Satnoianu, Phys. Rev. E **71**, 015204(R) (2005).
[25] D. G. Míguez, R. A. Satnoianu, and A. P. Muñuzuri, Phys. Rev. E (to be published).
[26] M. Kærn, R. Satnoianu, A. P. Muñuzuri, and M. Menzinger, Phys. Chem. Chem. Phys. **4**, 1319 (2002).
[27] A. P. Muñuzuri, M. Dolnik, A. M. Zhabotinsky, and I. R. Epstein, J. Am. Chem. Soc. **121**, 8055 (1999).
[28] A. K. Horváth, M. Dolnik, A. P. Muñuzuri, A. M. Zhabotinsky, and I. R. Epstein, Phys. Rev. Lett. **83**, 2950 (1999).
[29] V. Casets, E. Dulos, J. Boissonade, and P. De Kepper, Phys. Rev. Lett. **64**, 2953 (1990).
[30] J. Boissonade, E. Dulos, and P. de Kepper, in *Chemical Waves and Patterns*, edited by R. Kapral and Kennet Showalter (Kluwer Acamemic, Amsterdam, 1995), p. 221.
[31] I. Lengyel, G. Rábai, and I. R. Epstein, J. Am. Chem. Soc. **112**, 9104 (1990).
[32] B. Rudovics, E. Barillot, P. Davies, E. Dulos, J. Boissonade, and P. De Kepper, J. Phys. Chem. **103**, 1790 (1999).
[33] A. Sanz-Anchelergues and A. P. Muñuzuri, Int. J. Bifurcation Chaos Appl. Sci. Eng. **11**, 2739 (2000).
[34] O. A. Nekhamkina, A. A. Nepomnyashchy, B. Y. Rubinstein, and M. Sheintuch, Phys. Rev. E **61**, 2436 (2000).
[35] O. Nekhamkina and M. Sheintuch, Phys. Rev. E **66**, 016204 (2002).
[36] J. R. Bamforth, S. Kalliadasis, J. H. Merkin, and S. K. Scott, Phys. Chem. Chem. Phys. **2**, 4013 (2000).